Driving Enhanced Quantum Sensing in Partially Accessible Many-Body Systems

Utkarsh Mishra* and Abolfazl Bayat†
Institute of Fundamental and Frontier Sciences, University of Electronic Science and Technology of China, Chengdu 610054, China

(Received 22 October 2020; accepted 26 July 2021; published 20 August 2021)

The ground-state criticality of many-body systems is a resource for quantum-enhanced sensing, namely, the Heisenberg precision limit, provided that one has access to the whole system. We show that, for partial accessibility, the sensing capabilities of a block of spins in the ground state reduces to the sub-Heisenberg limit. To compensate for this, we drive the Hamiltonian periodically and use a local steady state for quantum sensing. Remarkably, the steady-state sensing shows a significant enhancement in precision compared to the ground state and even achieves super-Heisenberg scaling for low frequencies. The origin of this precision enhancement is related to the closing of the Floquet quasienergy gap. It is in close correspondence with the vanishing of the energy gap at criticality for ground-state sensing with global accessibility. The proposal is general to all the integrable models and can be implemented on existing quantum devices.

DOI: 10.1103/PhysRevLett.127.080504

Introduction.—The high sensitivity of quantum systems to variations of their environment makes them superior sensors to their classical counterparts [1–8]. This is reflected in the Cramér-Rao inequality, which determines the precision limit of estimating an unknown field h, quantified by the standard deviation δh, through $\delta h \geq 1/\sqrt{MF}$, where M is the number of samples and F is the Fisher information [9,10]. While the classical Fisher information scales as $F_C \sim N$ (standard limit), with N being the number of resources (e.g., number of particles) in the sensor, the quantum mechanics allows us to go beyond this and achieve $F_Q \sim N^2$ (Heisenberg limit). Several quantum features are known to provide enhanced sensing precision: (i) entanglement in the special form of Greenberger-Horne-Zeilinger [11–15] or N00N [16–18] states, (ii) wave function collapse resulted from sequential measurements separated by intervals of free evolution [19–25], and (iii) quantum criticality in many-body systems [26–32]. Any of these approaches have their advantages and disadvantages. If a d-dimensional many-body system operates near its critical ground state, the quantum Fisher information (QFI) of the *whole* system scales as $F_Q \sim N^{2/d\nu}$, where the ν characterizes the critical exponent for the divergence of the correlation length [33]. In the absence of global accessibility, one can only control a subsystem, which, in general, is a mixed state. A key question is how QFI scales with the subsystem size in a critical system. Besides, can the Heisenberg scaling be retrieved if the scaling becomes sub-Heisenberg, due to the mixedness of the subsystem?

Nonequilibrium dynamics of periodically driven many-body systems has been exploited for investigating the emergence of steady state [34], time crystals [35], topological systems [36,37], entanglement generation [38–42], Floquet spectroscopy [43,44], dynamically controlled quantum thermometry [45], and dynamical phase transitions [46–48]. The useful features of periodically driven many-body systems are that (i) any local subsystem reaches a steady state, and (ii) the Floquet mechanism is applicable, which simplifies the study of the dynamics. In nonintegrable systems, a periodic field drives any small subsystem to a featureless infinite temperature thermal steady state with no memory of the Hamiltonian parameters [49]. On the other hand, for integrable models, a nontrivial steady state can be obtained that carries information about the Hamiltonian parameters [34,38–42,50–52]. An important, yet unexplored, open question is whether the local steady states of periodically driven integrable systems can be used for enhancing the sensing precision in many-body sensors with partial accessibility.

In this Letter, we address the above open problems by considering an XY spin chain for detecting a transverse magnetic field. We first find that, in the absence of global accessibility, the sensing precision, even at the critical point, diminishes to sub-Heisenberg scaling. Then, we show that by applying a proper periodic transverse field and exploiting the local steady states we can even achieve super-Heisenberg sensitivity. Remarkably, this enhanced sensing is not limited to the critical points of the system and exists for all the points across the phase diagram with a vanishing Floquet quasienergy gap. The protocol can be realized in existing quantum devices using simple measurements.

Model.—We consider quantum XY spin chain for measuring an unknown static transverse magnetic field h_0. To manipulate the system for the desired accuracy, we apply a

periodic transverse field $h(t)$ to the system. Therefore, the total Hamiltonian can be written as

$$H(t) = -\frac{J}{2}\sum_{i=1}^{N}\left[\left(\frac{1+\gamma}{2}\right)\sigma_i^x\sigma_{i+1}^x + \left(\frac{1-\gamma}{2}\right)\sigma_i^y\sigma_{i+1}^y\right] - \frac{[h_0+h(t)]}{2}\sum_i \sigma_i^z, \quad (1)$$

where $\sigma^\Theta(\Theta = x, y, z)$ are the Pauli matrices, J (which is set to be one throughout the Letter) is the exchange coupling, $-1 \le \gamma \le 1$ is the anisotropic parameter, and the periodic-boundary conditions, i.e., $\sigma_{N+1}^\alpha \equiv \sigma_1^\alpha$, is imposed. At time $t = 0$, a periodic field of the form of $h(t) = h_1 \sin(\omega t)$ is applied to the system, where $\omega = 2\pi/\tau$ with τ being the time period. The Hamiltonian $H(0)$ shows quantum criticality at $h_0 = h_c$ such that $h_c/J = 1$ for all values of γ [53]. We consider that system is initially prepared in the ground state of $H(0)$. However, as discussed in the Supplemental Material [54], the proposed mechanism is general and works for other initial states. By switching the probe field $h(t)$, the initial state starts to evolve. The exact solution for the evolved is provided in the Supplemental Material.

Sensing with global accessibility.—If one has access to the whole system, namely, $|\Psi_0(t)\rangle$, then the QFI is given by $F_Q(t) = 4\chi_F(t)$, where $\chi_F(t) = \langle\partial_{h_0}\Psi(t)|\partial_{h_0}\Psi(t)\rangle - |\langle\Psi(t)|\partial_{h_0}\Psi(t)\rangle|^2$. Especially for $H(0)$ the global QFI has been extensively studied and it was shown that at the ground-state criticality it scales as $F_Q^{gs} = F_Q(0) \sim N^2$ [26–31,33,59–65], while away from the criticality it scales as $F_Q^{gs} = F_Q(0) \sim N$. We show this in the Supplemental Material by simulating the QFI of the global system. In the rest of the Letter, we focus on partial accessibility.

Sensing with partial accessibility.—In the absence of global accessibility, one has to rely on accessing a local block of size L with $L \ll N$. The partially accessible state of the system is described by the reduced density matrix obtained by tracing out all particles out of the block L, namely, $\rho_L(t) = \mathrm{tr}_{N-L}(|\Psi_0(t)\rangle\langle\Psi_0(t)|)$. The QFI of the state is given by [10]

$$F_Q = \sum_{r,s=1}^{2^L} \frac{2\mathrm{Re}(\langle\lambda_r|\partial_{h_1}\rho_L|\lambda_s\rangle\langle\lambda_s|\partial_{h_1}\rho_L|\lambda_r\rangle)}{\lambda_r + \lambda_s}, \quad (2)$$

where $\rho_L = \sum_{r=1}^{2^L}\lambda_r|\lambda_r\rangle\langle\lambda_r|$ with λ_r and $|\lambda_r\rangle$ being the eigenvalues and eigenvectors of ρ_L, respectively. Re[·] denotes the real parts of the quantity inside the parenthesis and the sum excludes terms for which $\lambda_r + \lambda_s = 0$. Note that the QFI is independent of the choice of the measurement operators and, in general, depends on the unknown parameter h_0. Calculation of the QFI for the state ρ_L is given in the Supplemental Material [54].

Steady state of a block.—After a long time t, the reduced density matrix $\rho_L(t)$ equilibrates to a steady state. Our goal in this Letter is to measure the QFI for such a steady state. By using $H(t+\tau) = H(t)$ and Floquet formalism, one can obtain the time-evolved state after n cycles from an initial state $|\Psi_0\rangle$ as $|\Psi(n\tau)\rangle = \sum_i e^{-i\mu_i n\tau}|\mu_i\rangle\langle\mu_i|\Psi_0\rangle$. Here $\{\mu_i, |\mu_i\rangle\}$ are the eigenvalues (Floquet quasienergies) and eigenvectors of the one-period Floquet operator $U(\tau) = \mathcal{T}e^{-i\int_0^\tau H(t)dt}$, with $\mathcal{T}$ being time-order operator. The expectation value of a local operator $\mathcal{O}$ in the time-evolved state then can be expressed as $\langle\mathcal{O}\rangle = \sum_\ell\langle\mu_\ell|\mathcal{O}|\mu_\ell\rangle|\langle\mu_\ell|\Psi_0\rangle|^2 + \sum_{\ell\neq j}\langle\mu_\ell|\mathcal{O}|\mu_j\rangle\langle\mu_\ell|\Psi_0\rangle\langle\Psi_0|\mu_j\rangle e^{-2i(\mu_\ell-\mu_j)n\tau}$. The first and second terms describe the diagonal contribution and the fluctuation around the diagonal term, respectively. The second term vanishes for a long time (Riemann-Lebesgue lemma). Using the above formalism, we calculate the expectation value of the fermionic correlation functions in the limit $t \to \infty$. (See Supplemental Material for obtaining the local steady state of the model [54].) These correlation functions give the steady-state QFI, namely, $F_Q^{ss} = \lim_{t\to\infty} F_Q(t)$ for the state ρ_L.

Ground-state sensing.—In the absence of global accessibility, one has to rely on the sensing capability of ρ_L, which, in general, is a mixed state. This mixedness can diminish the sensing capability. To quantify this, we consider the ground state of $H(0)$ for $N = 6000$ and plot the QFI, namely, F_Q^{gs}, for $L = 2$ and $L = 4$ in Figs. 1(a) and 1(b), respectively. It can be seen from the plots that F_Q^{gs} shows peaks at points $h_0/J = \pm 1$ that marks the quantum

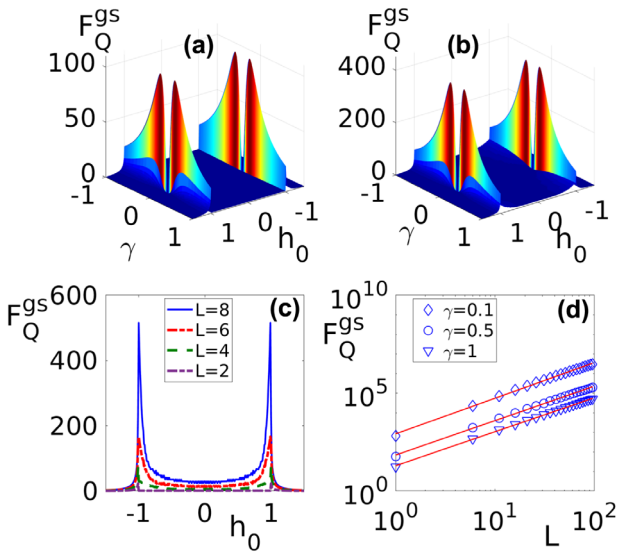

FIG. 1. The QFI of the ground state F_Q^{gs} as a function of γ and h_0 for (a) $L = 2$ and (b) $L = 4$. (c) The F_Q^{gs} as a function of h_0 when $\gamma = 1$ for various choices of L. (d) The log-log scaling of F_Q^{gs} as a function of L for different γ's. The fitting is shown by the regular line, whereas the markers represent the original data. In all panels $N = 6000$.

criticality of the system. It is an interesting observation that not only the QFI of a full chain but also that of the reduced state distinguishes the criticality [26,31,66–68]. In Figs. 1(a) and 1(b), the F_Q^{gs} becomes vanishingly small at $\gamma = 0$. Since for $\gamma = 0$, the field part of $H(0)$ commutes with the interaction part, the variation of the field h_0 does not induce any change in the ground state of $H(0)$, which reflects itself in $F_Q^{gs} = 0$. To have a better understanding of the role of L, we plot F_Q^{gs} versus h_0 at $\gamma = 1$ in Fig. 1(c) for various L's. The QFI increases with L and this effect becomes even more pronounced at the critical point $h_0/J = \pm 1$. To have a quantitative analysis for the scaling of the QFI at the critical point, in Fig. 1(d) we plot F_Q^{gs} as a function of L for $\gamma = 0.1$, 0.5, and 1 by fixing $h_0/J = 1$. The scaling follows a power-law form, i.e., $F_Q^{gs}(h = h_c) \sim aL^{\eta}$. Numerical fitting results in $(a, \eta) = (6.718, 1.8)$ for $\gamma = 0.1$, $(a, \eta) = (4.2235, 1.76)$ for $\gamma = 0.5$, and $(a, \eta) = (2.967, 1.74)$ for $\gamma = 1$, respectively. Thus, for the critical ground state and with partial accessibility, the QFI scales weaker than the Heisenberg bound (i.e., $\eta = 2$), although it still outperforms the standard limit (i.e., $\eta = 1$) showing quantum-enhanced sensing. Is it possible to improve this and retrieve Heisenberg scaling?

Steady-state sensing.—To enhance the sensing capability with $\rho_L(t)$, we propose to apply a periodic drive as given in Eq. (1). The resulting dynamics tend to thermalize the quantum state of the block. In nonintegrable systems, while the global quantum state can still be used for quantum sensing [69,70], the subsystems equilibrate to an infinite temperature state and carry no information about the Hamiltonian [49]. In integrable models, as in Eq. (1), the steady state does *not* thermalize to the infinite temperature due to local conserved quantities and thus carries a wealth of information about the parameters of the system [34]. To find the sensing capability of the steady state of a block of $L = 4$, in Figs. 2(a) and 2(b) we plot $F_Q(n\tau)$ as a function of time $t = n\tau$ for $\omega = 1$ and 4, respectively. The QFI reaches an equilibrium after a short transition time. Equilibration of the probe state is of multifold importance: (i) the imprinted information of h_0 in the density matrix may enhance the sensitivity and (ii) the emergent steady state remains almost fixed in time, which simplifies the measurement.

To see the sensing capability of the steady state for a choice of $h_1 = 1.5$ and $L = 4$, we compute the steady-state QFI, denoted as F_Q^{ss}. In Fig. 2(c), we plot F_Q^{ss} as a function of γ and h_0 for $\omega = 4$. The F_Q^{ss} shows similar behavior as F_Q^{gs} in Figs. 1(a) and 1(b), except around $\gamma = 0$ (the behavior of F_Q^{ss} as a function of γ is discussed in the Supplemental Material [54]). In Fig. 2(d), we plot the F_Q^{ss} for a lower frequency ($\omega = 2$). Interestingly, the F_Q^{ss} becomes nonzero along the line $h_0 = 0$, whereas it is zero for $\omega = 4$. Thus, by properly driving the system, extra peaks appear in the QFI even away from the ground-state

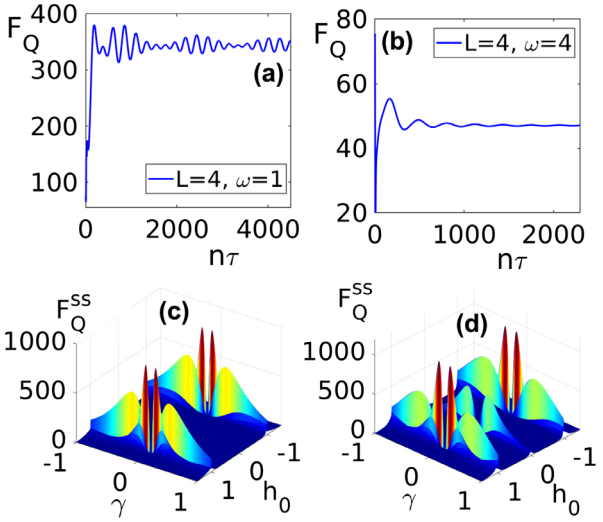

FIG. 2. F_Q as a function of time $t = n\tau$ for (a) $\omega = 1$, (b) $\omega = 4$ for $L = 4$, $h_0/J = 1$, and $\gamma = 1$. Steady state F_Q^{ss} as a function of h_0 and γ for (c) $\omega = 4$ and (d) $\omega = 2$. (a)–(d) The system size is $N = 6000$ and $h_1 = 1.5$.

criticality and thus achieve quantum-enhanced sensing over a wider range.

Floquet resonance.—To investigate the emergence of extra peaks, we fix the parameters $\gamma = 1$ and $h_1 = 1$ and plot the F_Q^{ss} as a function of h_0 in Figs. 3(a) and 3(b) for frequencies $\omega = 1$ and $\omega = 0.5$, respectively. In each panel, the different curves are for different block size L. It can be seen clearly from the plots that the number of peaks increases as the frequency gets smaller. The peaks are related to the eigenvalues of the one-period Floquet operator $U_k(\tau)$, where $U_k(\tau)$ is the Floquet operator for each quasimomentum mode $k \in [0, \pi]$, as discussed in the Supplemental Material [54]. The eigenvalues

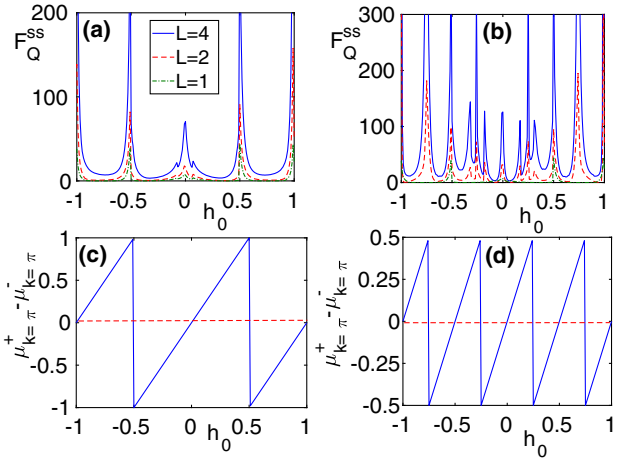

FIG. 3. The QFI in the steady state with respect to h_0 for different frequencies: (a) $\omega = 1$ and (b) $\omega = 0.5$. The difference of Floquet quasienergies $\mu^{\pm}_{k=\pi}$ for frequencies: (c) $\omega = 1$ and (d) $\omega = 0.5$. (a)–(d) $N = 6000$, $h_1 = 1.5$, and $\gamma = 1$.

of $U_k(\tau)$ can be written as $e^{i\tau\mu_k^{\pm}}$, where $\mu_k^{\pm} = \pm(\omega/\pi)\tan^{-1}\sqrt{1-\mathrm{Re}[u_k(\tau)]/1+\mathrm{Re}[u_k(\tau)]}$ are the Floquet quasienergies [34]. Interestingly, the peaks occur at the position of Floquet resonances, i.e., when $\mu_k^+ = \mu_k^-$. For $h_1 \neq 0$, the quasienergy spectrum shows avoided crossing except at $k = 0$ and $k = \pi$. Thus, the Floquet resonance condition will only be satisfied by modes at $k = 0$ and $k = \pi$. Therefore, the Floquet resonance condition for the energy eigenvalues becomes $2E_{k=0,\pi}(t = 0) = q\omega$ for some integer q, where $E_k(t = 0) = \pm\sqrt{[h_0 - J\cos(k)]^2 + J^2\gamma^2\sin(k)^2}$ (see the Supplemental Material for definition of E_k). We depict the behavior of the Floquet quasienergy gap, i.e., $\mu_{k=\pi}^+ - \mu_{k=\pi}^-$, as a function of h_0 for $\omega = 1$ and $\omega = 0.5$ in Figs. 3(c) and 3(d), respectively. It can be seen that, for each peak in Figs. 3(a) and 3(b), the quasienergy gap vanishes at those h_0. Thus, the vanishing of the quasienergy gap is responsible for the peaks in the F_Q^{ss} observed in Figs. 3(a) and 3(b). The detailed calculation of Floquet formalism and quasienergy gap is provided in the Supplemental Material [54].

Driving-enhanced sensing.—As seen above, driving the system can enhance the steady-state QFI. It is of utmost interest to see whether this can improve the scaling of the QFI as a function of L. We first focus on the critical point, i.e., $h_0/J = 1$, and without loss of generality fix the parameters $\gamma = 1$ and $h_1 = 1.5$. In Figs. 4(a)–4(c) we plot F_Q^{ss} versus L together with a power-law fitting function $\tilde{F}_Q^{ss} \sim aL^{\eta}$ at $h_0/J = 1$ for different frequencies such that $F_Q^{ss} \approx \tilde{F}_Q^{ss}$. The coefficient η shows that in the range $\omega \leq 2$ the scaling of the steady state surpasses the scaling of the ground state. Remarkably, by tuning the driving frequency to $\omega = 2$, see Fig. 4(a), one can indeed retrieve the Heisenberg scaling. Further decreasing the frequency can lead to the remarkable super-Heisenberg scaling of $\eta > 2$, shown in Figs. 4(b) and 4(c). This driving-enhanced sensitivity is not limited to the critical point. In Fig. 4(d), we depict the scaling of the QFI versus the block size L for $\omega = 1$ at $h_0/J = 0.5$, where the F_Q^{ss} peaks due to Floquet resonance, see Fig. 3(a). Interestingly, the scaling ($\eta = 1.8$) exceeds the standard quantum limit showing that quantum-enhanced sensing can be achieved at all Floquet resonances.

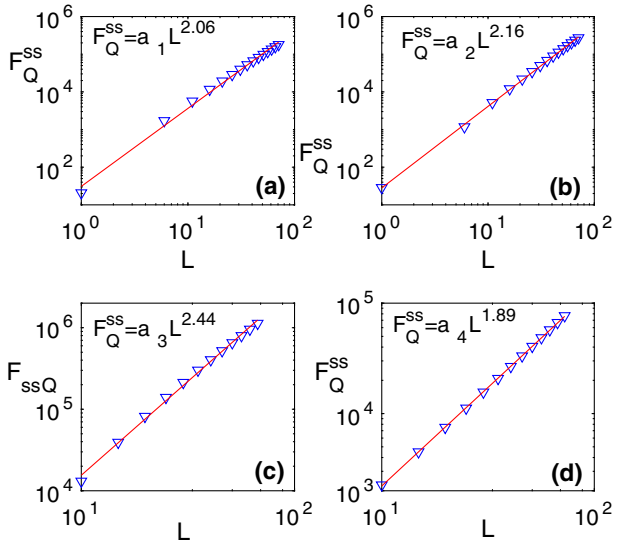

FIG. 4. Scaling of the F_Q^{ss} versus L along the vanishing Floquet quasienergy gap line for (a) $(\omega, h_0) = (2, 1)$, (b) $(\omega, h_0) = (1, 1)$, (c) $(\omega, h_0) = (0.5, 1)$, and (d) $(\omega, h_0) = (1, 0.5)$. The coefficients are $a_1 = 3.43$, $a_2 = 3.33$, $a_3 = 3.78$, and $a_4 = 3.15$. (a)–(d) $\gamma = 1$, $h_1 = 1.5$.

Role of the frequency.—As discussed earlier, the enhanced precision is directly related to the vanishing quasienergy gap, which is a function of the frequency of the driving field. In fact, the frequency ω has two roles. First, for $\omega < 2$, the QFI shows extra peaks that are absent in the phase diagram of the ground state, e.g., see Fig. 2(d). Second, at the vanishing Floquet quasienergy gap points, lowering the ω results in better scaling. For instance, as shown in Figs. 4(a)–4(c), for the critical field $h_0 = 1$ one can achieve super-Heisenberg scaling once $\omega < 1$.

Realization in near-term quantum simulators.—Among the emerging quantum simulators, ion traps [71–73] and superconducting devices [74–76] are the best candidates for the realization of our protocol, as their interaction can be described by the Hamiltonian in Eq. (1). Near-term quantum devices and simulators are limited in size [77]. To investigate the performance of our protocol on small systems, in Fig. 5(a) we plot F_Q for a block of size $L = 4$ as a function of time for various total system sizes. Interestingly, small systems provide high quantum Fisher information, indicating more potential for sensing. This is because the larger the system, the more degrees of freedom for the dispersion of information.

It is worth emphasizing that F_Q provides an ultimate bound for sensing precision attained only if the measurement basis is optimal. However, the optimal measurement basis might be complicated and depends on the unknown parameter that makes the saturation of the Cramér-Rao bound very challenging. Here, we consider a simple (but nonoptimal) block magnetization measurement along the

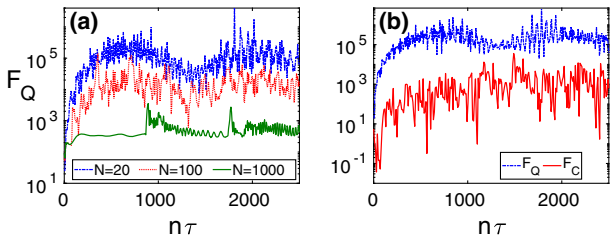

FIG. 5. (a) Dynamics of QFI for different system size N and fixed block size $L = 4$. (b) Dynamics of both quantum and classical Fisher information of a block of $L = 4$ for a system of size $N = 14$. (a),(b) $h_0 = 1, \gamma = 1$, $h_1 = 1.5$, and $\omega = 1$.

x direction and compute its corresponding classical Fisher information F_C (the definition of F_C is in the Supplemental Material [54]). In Fig. 5(b), we plot both F_C and F_Q for a block of size $L = 4$ as a function of time in a system of length $N = 14$. Interestingly, the F_C not only follows the behavior of F_Q but also takes high values. It shows that a simple nonoptimal measurement can serve for sensing.

Conclusion.—In this Letter, we have shown that, in the absence of global accessibility of the whole state, the Heisenberg scaling of the QFI for the critical many-body ground states of integrable systems reduces to sub-Heisenberg. To retrieve the Heisenberg scaling, we proposed to drive the system using a periodic field and use the steady state of a block for sensing. Our results show that, by tuning the frequency of the periodic field, one can generate multiple peaks across the phase diagram, improving the sensing over a larger interval. The scaling at all these peaks exceeds the standard limit precision and shows significant enhancement compared to the ground state. Remarkably, at lower frequencies, one can even achieve super-Heisenberg scaling for the QFI. This steady-state quantum-enhanced sensitivity can be explained by the closing of the Floquet quasienergy gap. The protocol is general to all integrable models and best suited for ion traps and superconducting devices in which even a simple nonoptimal measurement, such as block magnetization, can be used for achieving high precision.

A. B. thanks the National Key R&D Program of China (Grant No. 2018YFA0306703) and National Science Foundation of China (Grants No. 12050410253 and No. 92065115) for their support. U. M. acknowledges funding from the Chinese Postdoctoral Science Fund 2018M643437.

*Corresponding author.
utka4345@gmail.com, utkarsh.mishra@uestc.edu.cn
†Corresponding author.
abolfazl.bayat@uestc.edu.cn

[1] M. Oszmaniec, R. Augusiak, C. Gogolin, J. Kołodyński, A. Acín, and M. Lewenstein, Random Bosonic States for Robust Quantum Metrology, Phys. Rev. X **6**, 041044 (2016).
[2] C. Degen, F. Reinhard, and P. Cappellaro, Quantum sensing, Rev. Mod. Phys. **89**, 035002 (2017).
[3] D. Braun, G. Adesso, F. Benatti, R. Floreanini, U. Marzolino, M. W. Mitchell, and S. Pirandola, Quantum enhanced measurements without entanglement, Rev. Mod. Phys. **90**, 035006 (2018).
[4] L. Pezzé, A. Smerzi, M. K. Oberthaler, R. Schmied, and P. Treutlein, Quantum metrology with nonclassical states of atomic ensembles, Rev. Mod. Phys. **90**, 035005 (2018).
[5] K. Y. Yip, K. On Ho, K. Y. Yu, Y. Chen, W. Zhang, S. Kasahara, Y. Mizukami, T. Shibauchi, Y. Matsuda, S. K. Goh, and S. Yang, Quantum sensing of local magnetic field texture in strongly correlated electron systems under extreme conditions, Science **366**, 1355 (2019).
[6] A. Kuwahata, T. Kitaizumi, K. Saichi, T. Sato, R. Igarashi, T. Ohshima, Y. Masuyama, T. Iwasaki, M. Hatano, F. Jelezko, M. Kusakabe, T. Yatsui, and M. Sekino, Magnetometer with nitrogen-vacancy center in a bulk diamond for detecting magnetic nanoparticles in biomedical applications, Sci. Rep. **10**, 2483 (2020).
[7] J. Smits, J. T. Damron, P. Kehayias, A. F. McDowell, N. Mosavian, I. Fescenko, N. Ristoff, A. Laraoui, A. Jarmola, and V. M. Acosta, Two-dimensional nuclear magnetic resonance spectroscopy with a microfluidic diamond quantum sensor, Sci. Adv. **5**, eaaw7895 (2019).
[8] J. Casanova, E. Torrontegui, M. B. Plenio, J. J. García-Ripoll, and E. Solano, Modulated Continuous Wave Control for Energy-Efficient Electron-Nuclear Spin Coupling, Phys. Rev. Lett. **122**, 010407 (2019).
[9] S. L. Braunstein and C. M. Caves, Statistical Distance and the Geometry of Quantum States, Phys. Rev. Lett. **72**, 3439 (1994).
[10] M. G. A. Paris, Quantum estimation for quantum technology, Int. J. Quantum. Inform. **07**, 125 (2009).
[11] V. Giovannetti, S. Lloyd, and L. Maccone, Quantum-enhanced measurements: Beating the standard quantum limit, Science **306**, 1330 (2004).
[12] V. Giovannetti, S. Lloyd, and L. Maccone, Quantum Metrology, Phys. Rev. Lett. **96**, 010401 (2006).
[13] F. Fröwis and W. Dür, Stable Macroscopic Quantum Superpositions, Phys. Rev. Lett. **106**, 110402 (2011).
[14] D. Dobrzanski, J. Kołodyński, and M. Guta, The elusive Heisenberg limit in quantum enhanced metrology, Nat. Commun. **3**, 1063 (2012).
[15] H. Kwon, K. C. Tan, T. Volkoff, and H. Jeong, Nonclassicality as a Quantifiable Resource for Quantum Metrology, Phys. Rev. Lett. **122**, 040503 (2019).
[16] J. P. Dowling, Quantum optical metrology–the lowdown on high-N00N states, Contemp. Phys. **49**, 125 (2008).
[17] J. Joo, W. J. Munro, and T. P. Spiller, Quantum Metrology with Entangled Coherent States, Phys. Rev. Lett. **107**, 083601 (2011).
[18] S. Slussarenko, M. M. Weston, H. M. Chrzanowski, L. K. Shalm, V. B. Verma, S. W. Nam, and G. J. Pryde, Unconditional violation of the shot-noise limit in photonic quantum metrology, Nat. Photonics **11**, 700 (2017).
[19] C. Bonato, M. S. Blok, H. T. Dinani, D. W. Berry, M. L. Markham, D. J. Twitchen, and R. Hanson, Optimized quantum sensing with a single electron spin using real-time adaptive measurements, Nat. Nanotechnol. **11**, 247 (2016).
[20] R. S. Said, D. W. Berry, and J. Twamley, Nanoscale magnetometry using a single-spin system in diamond, Phys. Rev. B **83**, 125410 (2011).
[21] B. L. Higgins, D. W. Berry, S. D. Bartlett, H. M. Wiseman, and G. J. Pryde, Entanglement-free Heisenberg-limited phase estimation, Nature (London) **450**, 393 (2007).
[22] D. W. Berry, B. L. Higgins, S. D. Bartlett, M. W. Mitchell, G. J. Pryde, and H. M. Wiseman, How to perform the most accurate possible phase measurements, Phys. Rev. A **80**, 052114 (2009).
[23] B. L. Higgins, D. W. Berry, S. D. Bartlett, M. W. Mitchell, H. M. Wiseman, and G. J. Pryde, Demonstrating Heisenberg-limited unambiguous phase estimation without adaptive measurements, New J. Phys. **11**, 073023 (2009).

[24] S. Gammelmark and K. Mølmer, Remote Quantum Sensing with Heisenberg Limited Sensitivity in Many Body Systems, Phys. Rev. Lett. **112**, 170401 (2014).
[25] G. S. Jones, S. Bose, and A. Bayat, Remote quantum sensing with Heisenberg limited sensitivity in many body systems, arXiv:2003.02308.
[26] P. Zanardi and N. Paunković, Ground state overlap and quantum phase transitions, Phys. Rev. E **74**, 031123 (2006).
[27] P. Zanardi, H. T. Quan, X. Wang, and C. P. Sun, Mixed-state fidelity and quantum criticality at finite temperature, Phys. Rev. A **75**, 032109 (2007).
[28] P. Zanardi, M. G. A. Paris, and L. Campos Venuti, Quantum criticality as a resource for quantum estimation, Phys. Rev. A **78**, 042105 (2008).
[29] C. Invernizzi, M. Korbman, L. C. Venuti, and M. G. A. Paris, Optimal quantum estimation in spin systems at criticality, Phys. Rev. A **78**, 042106 (2008).
[30] M. Skotiniotis, P. Sekatski, and W. Dür, Quantum metrology for the Ising Hamiltonian with transverse magnetic field, New J. Phys. **17**, 073032 (2015).
[31] S.-J. Gu, Fidelity approach to quantum phase transitions, Int. J. Mod. Phys. B **24**, 4371 (2010).
[32] S. Gammelmark and K. Mølmer Phase transitions and Heisenberg limited metrology in an Ising chain interacting with a single-mode cavity field, New J. Phys. **13**, 053035 (2011).
[33] M. M. Rams, P. Sierant, O. Dutta, P. Horodecki, and J. Zakrzewski, At the Limits of Criticality-Based Quantum Metrology: Apparent Super-Heisenberg Scaling Revisited, Phys. Rev. X **8**, 021022 (2018).
[34] A. Russomanno, A. Silva, and G. E. Santoro, Periodic Steady Regime and Interference in a Periodically Driven Quantum System, Phys. Rev. Lett. **109**, 257201 (2012).
[35] D. V. Else, B. Bauer, and C. Nayak, Floquet Time Crystals, Phys. Rev. Lett. **117**, 090402 (2016).
[36] M. S. Rudner, N. H. Lindner, E. Berg, and M. Levin, Anomalous Edge States and the Bulk-Edge Correspondence for Periodically Driven Two-Dimensional Systems, Phys. Rev. X **3**, 031005 (2013).
[37] M. Thakurathi, A. A. Patel, D. Sen, and A. Dutta, Floquet generation of Majorana end modes and topological invariants, Phys. Rev. B **88**, 155133 (2013).
[38] T. J. G. Apollaro, G. M. Palma, and J. Marino, Entanglement entropy in a periodically driven quantum Ising chain, Phys. Rev. B **94**, 134304 (2016).
[39] A. Russomanno, G. E. Santoro, and R. Fazio, Entanglement entropy in a periodically driven Ising chain, J. Stat. Mech. (2016) 073101.
[40] A. Sen, S. Nandy, and K. Sengupta, Entanglement generation in periodically driven integrable systems: Dynamical phase transitions and steady state, Phys. Rev. B **94**, 214301 (2016).
[41] S. Lorenzo, J. Marino, F. Plastina, G. M. Palma, and T. J. G. Apollaro, Quantum critical scaling under periodic driving, Sci. Rep. **7**, 5672 (2017).
[42] U. Mishra, R. Prabhu, and D. Rakshit, Quantum correlations in periodically driven spin chains: Revivals and steady-state properties, J. Magn. Magn. Mater. **491**, 165546 (2019).
[43] J. E. Lang, R. B. Liu, and T. S. Monteiro, Dynamical-Decoupling-Based Quantum Sensing: Floquet Spectroscopy, Phys. Rev. X **5**, 041016 (2015).
[44] J. V. Koski, A. J. Landig, A. Pályi, P. Scarlino, C. Reichl, W. Wegscheider, G. Burkard, A. Wallraff, K. Ensslin, and T. Ihn, Floquet Spectroscopy of a Strongly Driven Quantum Dot Charge Qubit with a Microwave Resonator, Phys. Rev. Lett. **121**, 043603 (2018).
[45] V. Mukherjee, A. Zwick, A. Ghosh, Xi Chen, and G. Kurizki, Enhanced precision bound of low-temperature quantum thermometry via dynamical control, Commun. Phys. **2**, 162 (2019).
[46] K. Yang, L. Zhou, W. Ma, Xi Kong, P. Wang, Xi Qin, X. Rong, Ya Wang, F. Shi, J. Gong, and J. Du, Floquet dynamical quantum phase transitions, Phys. Rev. B **100**, 085308 (2019).
[47] R. Jafari and A. Akbari, Floquet dynamical phase transition and entanglement spectrum, Phys. Rev. A **103**, 012204 (2021).
[48] S. Zamani, R. Jafari, and A. Langari, Floquet dynamical quantum phase transition in the extended *XY* model: Nonadiabatic to adiabatic topological transition, Phys. Rev. B **102**, 144306 (2020).
[49] K. Mallayya and M. Rigol, Heating Rates in Periodically Driven Strongly Interacting Quantum Many-Body Systems, Phys. Rev. Lett. **123**, 240603 (2019).
[50] T. Ishii, T. Kuwahara, T. Mori, and N. Hatano, Heating in Integrable Time-Periodic Systems, Phys. Rev. Lett. **120**, 220602 (2018).
[51] T. Brydges, A. Elben, P. Jurcevic, B. Vermersch, C. Maier, B. P. Lanyon, P. Zoller, R. Blatt, and C. F. Roos, Probing entanglement entropy via randomized measurements, Science **364**, 260 (2019).
[52] U. Mishra and A. Bayat, Integrable quantum many-body sensors for ac field sensing, arXiv:2105.13507.
[53] S. Sachdev, *Quantum Phase Transitions* (Cambridge University Press, Cambridge, England, 2017).
[54] See Supplemental Material at http://link.aps.org/supplemental/10.1103/PhysRevLett.127.080504 for (i) the analytical treatment of the time-dependent Hamiltonian, (ii) computing the quantum Fisher information, and (iii) investigating the role of the initial state, which contains Refs. [55–58].
[55] E. Lieb, T. Schultz, and D. Mattis, Two soluble models of an antiferromagnetic chain, Ann. Phys. (N.Y.) **16**, 407 (1961).
[56] P. Pfeuty, The one-dimensional Ising model with a transverse field, Ann. Phys. (N.Y.) **57**, 79 (1970).
[57] A. Carollo, B. Spagnolo, and D. Valenti, Symmetric logarithmic derivative of fermionic Gaussian states, Entropy **20**, 485 (2018).
[58] D. Šafránek, Discontinuities of the quantum Fisher information and the Bures metric, Phys. Rev. A **95**, 052320 (2017).
[59] L. Gong and P. Tong, Fidelity susceptibility, and von Neumann entropy to characterize the phase diagram of an extended Harper model, Phys. Rev. B **78**, 115114 (2008).
[60] D. Schwandt, F. Alet, and S. Capponi, Quantum Monte Carlo Simulations of Fidelity at Magnetic

Quantum Phase Transitions, Phys. Rev. Lett. **103**, 170501 (2009).
[61] A. F. Albuquerque, F. Alet, C. Sire, and S. Capponi, Quantum critical scaling of fidelity susceptibility, Phys. Rev. B **81**, 064418 (2010).
[62] A. Polkovnikov and V. Gritsev, Universal dynamics near quantum critical points, understanding quantum phase transitions, in *Understanding Quantum Phase Transitions*, edited by Lincoln D. Carr (Taylor & Francis, Boca Raton, 2010).
[63] B. Damski, Fidelity susceptibility of the quantum Ising model in a transverse field: The exact solution, Phys. Rev. E **87**, 052131 (2013).
[64] B. Damski and M. M. Rams, Exact results for fidelity susceptibility of the quantum Ising model: The interplay between parity, system size, and magnetic field, J. Phys. A **47**, 025303 (2014).
[65] A. Langari and A. T. Rezakhan, Quantum renormalization group for ground-state fidelity., New J. Phys. **14**, 053014 (2012).
[66] P. D. Sacramento, N. Paunković, and V. R. Vieira, Fidelity spectrum and phase transitions of quantum systems, Phys. Rev. A **84**, 062318 (2011).
[67] C.-Y. Park, M. Kang, C.-W. Lee, J. Bang, S.-W. Lee, and H. Jeong, Quantum macroscopicity measure for arbitrary spin systems and its application to quantum phase transitions, Phys. Rev. A **94**, 052105 (2016).
[68] W. C. Yu, Y. C. Li, P. D. Sacramento, and H.-Q. Lin, Reduced density matrix and order parameters of a topological insulator, Phys. Rev. B **94**, 245123 (2016).
[69] L. J. Fiderer and D. Braun, Quantum metrology with quantum-chaotic sensors, Nat. Commun. **9**, 1351 (2018).
[70] W. Liu, M. Zhuang, Bo Zhu, J. Huang, and C. Lee, Quantum metrology via chaos in a driven Bose-Josephson system, Phys. Rev. A **103**, 023309 (2021).
[71] C. Monroe, W. C. Campbell, E. E. Edwards, R. Islam, D. Kafri, S. Korenblit, A. Lee, P. Richerme, C. Senko, and J. Smith, in Quantum simulation of spin models with trapped ions, *Proceedings of the International School of Physics "Enrico Fermi," Course CLXXXIX*, edited by M. Knoop, I. Marzoli, and G. Morigi (Ios Pr Inc., 2015), pp. 169–187.
[72] J. I. Cirac and P. Zoller, Goals and opportunities in quantum simulation, Nat. Phys. **8**, 264 (2012).
[73] R. Blatt and C. F. Roos, Quantum simulations with trapped ions, Nat. Phys. **8**, 277 (2012).
[74] Q. Guo, C. Cheng, Z.-H. Sun, Z. Song, H. Li, Z. Wang, W. Ren, H. Dong, D. Zheng, Y. Zhang, R. Mondaini, H. Fan, and H. Wang, Observation of energy-resolved many-body localization, Nat. Phys. **17**, 234 (2021).
[75] M. Gong, G. D. Neto, C. Zha, Y. Wu, H. Rong, Y. Ye, S. Li, Q. Zhu, S. Wang, Y. Zhao, F. Liang, J. Lin, Y. Xu, C.-Z. Peng, H. Deng, A. Bayat, X. Zhu, and J.-W. Pan, Experimental characterization of quantum many-body localization transition, Phys. Rev. Research **3**, 033043 (2021).
[76] P. Roushan *et al.*, Spectroscopic signatures of localization with interacting photons in superconducting qubits, Science **358**, 1175 (2017).
[77] J. Preskill, Quantum computing in the NISQ era and beyond, Quantum **2**, 79 (2018).